Letters

A Novel Full-Bridge Step Density Modulation for Wireless Power Transfer Systems

Jiaqi Tang, Tuopu Na, and Qianfan Zhang, *Member, IEEE*

***Abstract*—Aiming for wireless power transfer (WPT) systems with high efficiency demands inverters under zero-voltage switching (ZVS) conditions. This letter presents a novel full-bridge step density modulation (FB-SDM) for WPT systems based on the step density averaging principle, which can achieve full-range ZVS operation. Compared with existing ZVS modulation schemes, such as pulse density modulation and hybrid frequency pacing, the proposed modulation scheme has the ability of balancing power device losses and the minimum low frequency output fluctuation. Simulation and experimental results prove that FB-SDM is one of the most potential ZVS modulation schemes for WPT systems.**

***Index Terms*—Hybrid frequency pacing (HFP), pulse density modulation (PDM), step density modulation (SDM), wireless power transfer (WPT), zero-voltage switching (ZVS).**

I. Introduction

MANY researchers aim to increase the efficiency of wireless power transfer (WPT) systems. Reducing the inverter losses is one of the efficient paths for increasing efficiency. The classical pulsewidth modulation (PWM) inverters operating at the resonant frequency of WPT systems suffer from hard switching problem, which generates large switching losses and electromagnetic interference [1]. Although variable frequency control could operate with zero-voltage switching (ZVS) condition, the reactive current increased the conduction losses.

A class of modulation schemes, such as pulse density modulation (PDM) [2], hybrid frequency pacing (HFP) [3], [4], and step density modulation (SDM) [5], have been proposed for resonant systems to achieve full-range ZVS and zero phase angle at the same time. PDM was the first to be presented for induction melting, which regulates the output power by varying the density of the pulses. PDM was also applied for WPT systems [6]. HFP utilizes the high-order harmonics of the square wave at a specific frequency to regulate the output power. The waveforms of HFP are similar to PDM, but the output power ripple of HFP is smaller than PDM. The SDM scheme splits a pulse into two steps and arranges these steps into a waveform, so that the density of the steps can regulate the output power. Although the waveforms of SDM are identical to those of HFP, the advantage of SDM is easier implement.

Manuscript received 15 June 2022; revised 13 July 2022 and 3 August 2022; accepted 14 August 2022. Date of publication 22 August 2022; date of current version 10 October 2022. *(Corresponding author: Tuopu Na.)*

The authors are with the School of Electrical Engineering and Automation, Harbin Institute of Technology, Harbin 150001, China (e-mail: tang_jiaqi@outlook.com; natuopu@126.com; zhang_qianfan@hit.edu.cn).

Color versions of one or more figures in this article are available at https://doi.org/10.1109/TPEL.2022.3200759.

Digital Object Identifier 10.1109/TPEL.2022.3200759

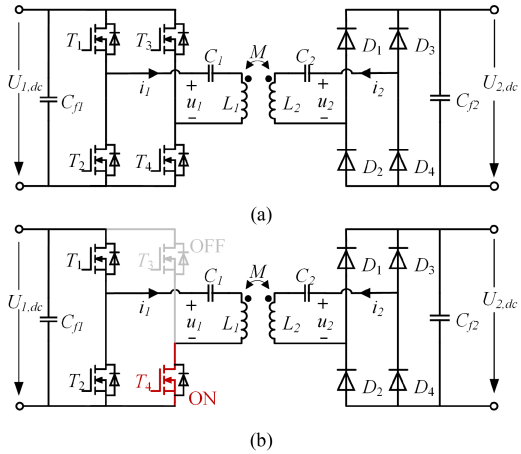

Fig. 1. Typical series–series compensated WPT system. (a) Full-bridge mode. (b) Half-bridge mode.

Except for achieving the ZVS condition, another advantage of this class of modulation schemes is that they can be applied in both full-bridge and half-bridge inverters. Therefore, some modulation schemes were proposed to further reduce the output power ripple on full-bridge inverters. They are called enhanced PDM (EPDM) [7]. EPDM is called improved PDM in WPT applications [8], [9]. The reduction of output ripple is achieved by switching the inverter from full-bridge mode to half-bridge mode, as shown in Fig. 1. Because the output voltage of half-bridge mode is only half of full-bridge mode, EPDM reduces twice the output ripple. However, EPDM brings a disadvantage, which is the imbalanced losses of the switching devices. As shown in Fig. 1(b), T_4 is twice the conduction loss of T_1 and T_2 in half-bridge mode, but the loss of T_3 is zero. It means that the required minimum rated current of T_4 is much larger than that of T_3.

This letter improves SDM for reducing the low-frequency ripple on full-bridge inverters. The proposed modulation scheme is named full-bridge SDM (FB-SDM). Compared with other ZVS modulation schemes, FB-SDM makes two breakthroughs as follows.

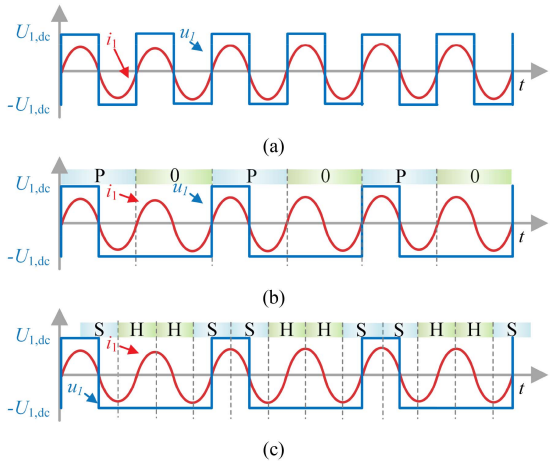

Fig. 2. Voltage and current waveforms of PDM and SDM. (a) $\delta = 1$. (b) PDM for $\delta = 0.5$. (c) SDM for $\delta = 0.5$.

1) FB-SDM has the minimum low-frequency output ripple.
2) The losses of power devices of the full-bridge inverter are more balanced in FB-SDM mode than in EPDM mode.

II. Reviews of PDM and SDM

A. Principle of PDM

PDM is a more common modulation scheme than SDM for WPT systems, so the principle of PDM is first briefly reviewed.

Fig. 2(a) depicts the voltage and currents waveforms of the inverter when the output power of WPT systems is maximum power. Only the fundamental component of square wave u_1 can generate power because of the bandpass characteristics of WPT systems. The output ratio δ can be defined to conveniently represent the average magnitude of the fundamental frequency component of u_1

$$\overline{u_{1(1)}} = \frac{4U_{1,\mathrm{dc}}}{\pi}\delta. \tag{1}$$

Therefore, $\delta = 1$ is the maximum average voltage of u_1, which is shown in Fig. 2(a). If half of the pulses in Fig. 2(a) are eliminated, the average value of output voltage will also be reduced by half. The PDM waveform for $\delta = 0.5$ is shown in Fig. 2(b). The period with a pulse is denoted as "P," and the period without a pulse is denoted as "0." Due to the resonant characteristics of WPT systems, the current can oscillate at the resonant frequency for several periods without pulses. Hence, the density of the pulses determines the average voltage of u_1, δ_{PDM} is given by

$$\delta_{\mathrm{PDM}} = \frac{N_P}{N_P + N_0} \tag{2}$$

where N_{P} and N_0 are the numbers of "P" periods and "0" periods, respectively. A more detailed principle of PDM can be found in [2] and [6].

B. Principle of SDM

The principle of SDM is very similar to that of PDM. In the view of SDM, the square wave can be divided by half-period, as shown in Fig. 2(c). The half-period with a level step is denoted as "S," and the half-period with a level hold is denoted as "H." Thus, the density of the steps can also determine the average voltage of u_1, δ_{SDM} is given by

$$\delta_{\mathrm{SDM}} = \frac{N_S}{N_S + N_H} \tag{3}$$

where N_{S} and N_{H} are the numbers of "S" half-periods and "H" half-periods, respectively.

Therefore, the average voltage of the waveform shown in Fig. 2(c) is also 0.5. The waveform of SDM is the same as that of PDM for $\delta = 0.5$. However, SDM has better performance at some output voltages. For example, Fig. 3 depicts the waveforms of PDM and SDM for $\delta = 1/3$. The current ripple of SDM is smaller because of the more even distribution of the steps. The basic element of SDM is the step whose duration is only half-period, so that the waveform arrangement of SDM is more flexible than that of PDM, which leads to the smaller output ripple of SDM.

The waveforms of HFP are the same as that of SDM. In the view of HFP, the frequency of square-wave voltage is one-third the current frequency in Fig. 3(b), and the third harmonic magnitude of the square-wave is one-third. Thus, the average voltage of u_1 at the current frequency component is one-third. The only

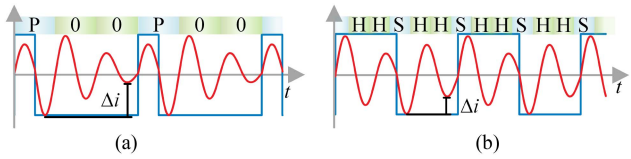

Fig. 3. Voltage and current waveforms of PDM and SDM for $\delta = 1/3$. (a) PDM. (b) SDM.

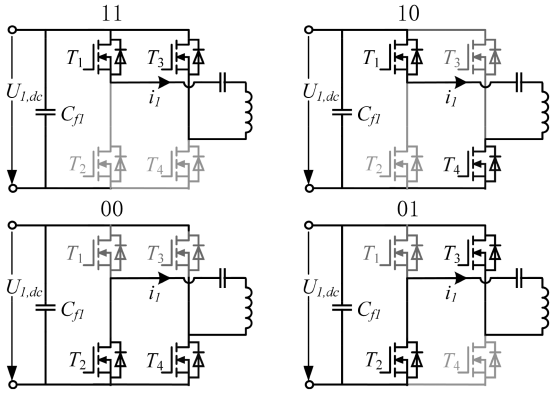

Fig. 4. Four switching modes of the full-bridge inverter.

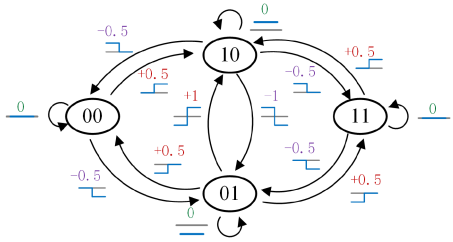

Fig. 5. Voltage steps generated by the state transitions.

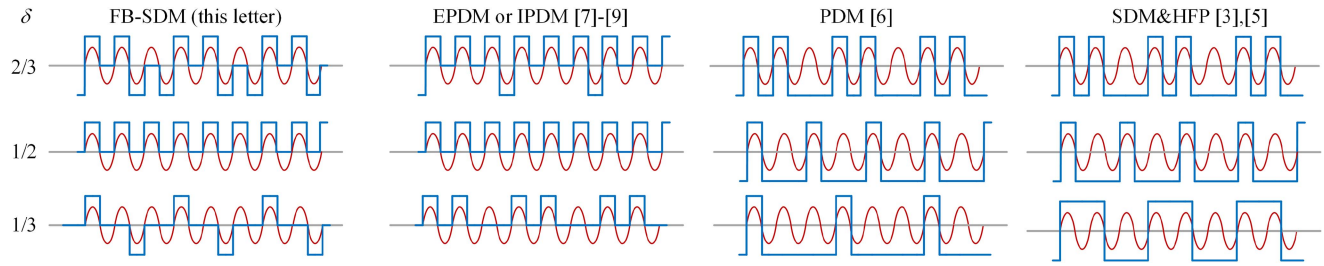

Fig. 6. Waveforms of FB-SDM and the other ZVS modulation.

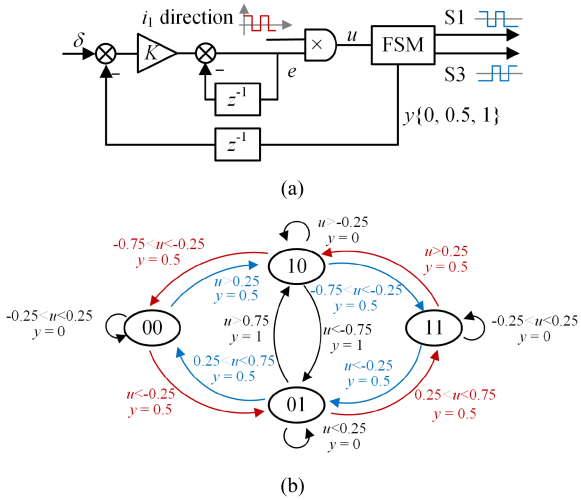

Fig. 7. Modulator for FB-SDM. (a) Structure. (b) State transition diagram of FB-SDM state machine.

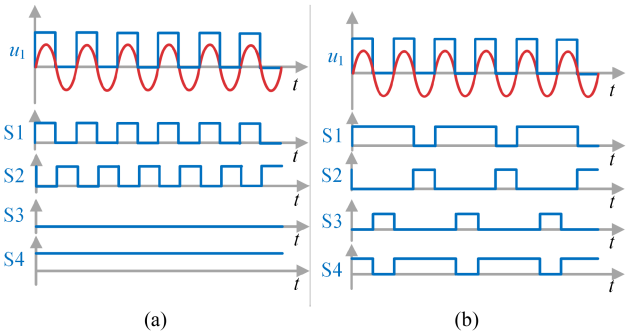

Fig. 8. Output waveforms and drive signals of two different state loops. (a) "10-00-10." (b) "10-00-10-11-10."

difference between HFP and SDM is the analytical perspective, and the implement of HFP is a bit complicated.

III. Principle of FB-SDM

EPDM utilizes the half-bridge mode of full-bridge inverters to reduce the low-frequency ripple. SDM can also use this characteristic, but the imbalanced losses of the power devices occur too. So, this letter abandons the perspective of mode selection and proposes the FB-SDM scheme to solve the problem of imbalanced losses.

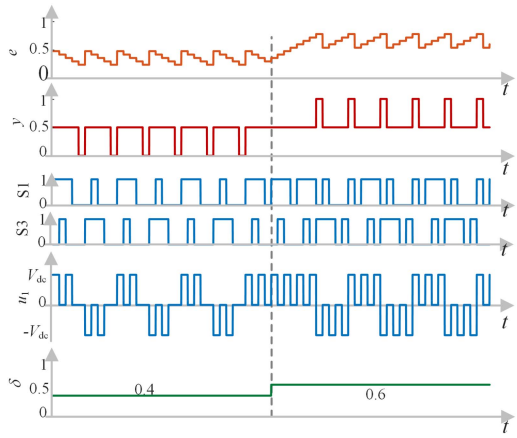

Fig. 9. Waveforms of FB-SDM modulator from $\delta = 0.4$ to $\delta = 0.6$.

Four valid switching modes of the full-bridge inverter are shown in Fig. 4. Apparently, the switching mode transitions can generate the voltage steps. All possible state transitions and corresponding voltage steps are shown in Fig. 5. The full-bridge inverter can generate three types of voltage steps: full-step, half-step, and level hold, which are denoted as "1," "0.5," and "0" in Fig. 5, respectively. The signs of these numbers only represent the step directions that should be the same as the directions of the current change.

As the principle of SDM, the average voltage of FB-SDM $\delta_{\text{FB-SDM}}$ can be given by

$$\delta_{\text{FB-SDM}} = \frac{N_{\text{FS}} + 0.5N_{\text{HS}}}{N_{\text{FS}} + N_{\text{HS}} + N_{\text{LH}}} \tag{4}$$

where N_{FS}, N_{HS}, and N_{LH} are the number of half-periods of full-step "1," half-step "0.5," and level hold "0," respectively.

Some typical waveforms of FB-SDM and the other ZVS modulation schemes are shown in Fig. 6. FB-SDM waveforms are symmetrical and the period is the shortest of all, so that the low-frequency ripple of FB-SDM is minimum.

Although the average voltage can be calculated by (4), it is still a problem to generate the FB-SDM waveform at any given δ. This letter proposes a modulator for FB-SDM, which is shown in Fig. 7. The modulator consists of a $\Sigma-\Delta$ modular, a multiplier, and a finite-state machine (FSM). The integrator output e multiplied by the sign of the current change direction is the FSM input u. The FB-SDM FSM is a Mealy machine and

TABLE I
PARAMETERS OF THE WPT SYSTEM

Symbol	Description	Value
L_1	Transmitter coil inductance	310.2 μH
L_2	Receiver coil inductance	286.3 μH
C_1	Transmitter compensated capacitance	11.5 nF
C_2	Receiver compensated capacitance	12.1 nF
M	Nominal mutual inductance	57.8 μH
N_{L1}, N_{L2}	Turns number of L_1 and L_2	25
D_1, D_2	Length of square coils	30 cm
d	Transfer distance	15 cm
f_{sw}	Switching frequency for $\delta = 1$	85 kHz
R_L	Rated load resistance	40 Ω
$U_{1,\mathrm{dc}}$	Input dc-link voltage	100 V
C_{f2}	DC filter capacitance	16 μF

with three output ports. The drive signals S1 and S3 only depend on the states. The feedback signal y depends on the transitions.

It should be noted that the states "10" and "01" have redundant transitions. For example, the functions of "10-00" and "10-11" are identical, and which transition is selected will not affect the output waveforms. However, the transition selection can affect the losses of power devices. Two different state loops are "10-00-10" and "10-00-10-11-10" for $\delta = 0.5$, of which the output waveforms and drive signals are shown in Fig. 8. The waveforms shown in Fig. 8(a) represent half-bridge mode of EPDM because the power device T_3 is OFF. The state loop "10-00-10-11-10" is with a better power losses balance.

This letter proposes a selection method for redundant transitions to balance the losses of four power devices. This criterion is to select the transition of the same color as last time when redundant transitions occur. Half-step transitions in Fig. 7(b) are colored blue or red. The blue transitions denote the inner loop and the red denote the outer loop. Avoiding switching between inner and outer loops can balance the losses of power devices.

Fig. 9 shows the waveforms of the FB-SDM modulator for $\delta = 0.4$ to 0.6. The step number $N_{\mathrm{FS}} = 2$ and $N_{\mathrm{HS}} = 8$ in an FB-SDM period correspond to the output voltage formula (4). The proposed FB-SDM modulator is valid for generating drive signals and balancing the losses.

IV. SIMULATION AND EXPERIMENTAL VERIFICATION

Based on the aforementioned analysis and design, some simulation and experimental results are given to verify the proposed FB-SDM. The system parameters are listed in Table I.

Fig. 10 shows the output waveforms and drive signals of EPDM and FB-SDM for $\delta = 0.4$. The drive signal S3 = 0 of EPDM means that the inverter works in the half-bridge mode, which causes the imbalanced losses of power devices. Each half-bridge of the inverter controlled by FB-SDM is in the switching state, so the losses of FB-SDM are more balanced. Furthermore, the low frequency ripple of FB-SDM is also smaller than that of EPDM, because the waveform arrangement of FB-SDM is more flexible.

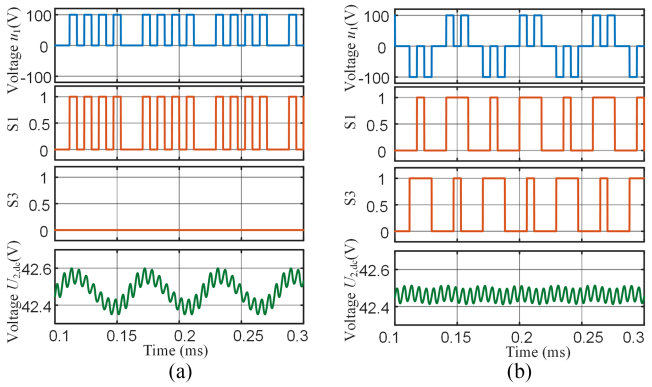

Fig. 10. Waveforms of EPDM and FB-SDM for $\delta = 0.4$. (a) EPDM. (b) FB-SDM.

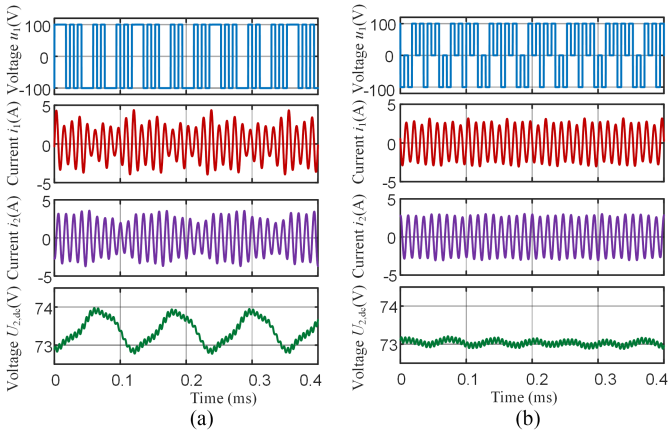

Fig. 11. Waveforms of SDM and FB-SDM for $\delta = 0.7$. (a) SDM. (b) FB-SDM.

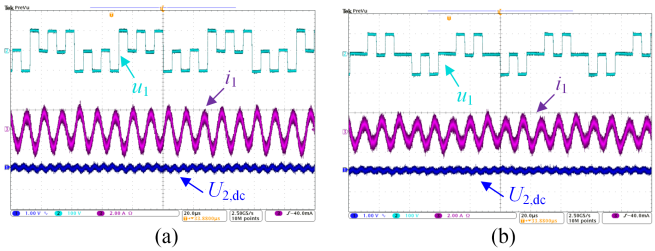

Fig. 12. Measured waveforms of FB-SDM. (a) $\delta = 0.6$. (b) $\delta = 0.4$. Scale: channel 2 u_1 100V/div, channel 3 i_1 2A/div, channel 1 $U_{2,\mathrm{dc}}$ 1V/div (ac coupling), time 20 μs/div.

Undoubtedly, FB-SDM performs better than PDM, because it has been proved in [7] that EPDM is better than PDM. The results of this letter are shown in Fig. 11. The peak-to-peak ripple of the output voltage $U_{2,\mathrm{dc}}$ in SDM mode is 1.3 V, but the ripple in FB-SDM mode is only 0.3 V.

The experimental results of FB-SDM modulation for $\delta = 0.6$ and $\delta = 0.4$ are shown in Fig. 12. The experimental results of the output ripple between the four modulations are shown in Fig. 13. The FB-SDM output voltage ripple is always minimum.

The system efficiency (dc to dc) is measured with a power analyzer (Yokogawa WT1800). The inverter is built with MOSFETs (IXFH80N20Q) and the rectifier is built with Schottky diodes (DSA120C150QB). The measured results are shown in

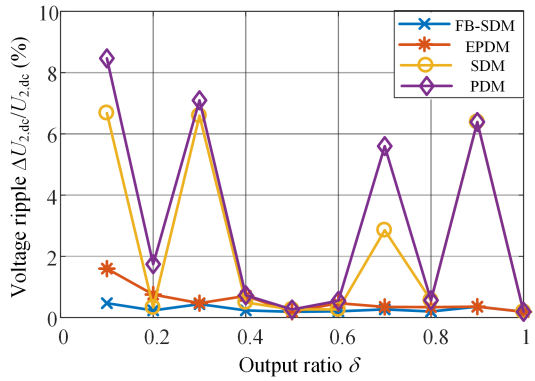

Fig. 13. Experimental output ripple comparison.

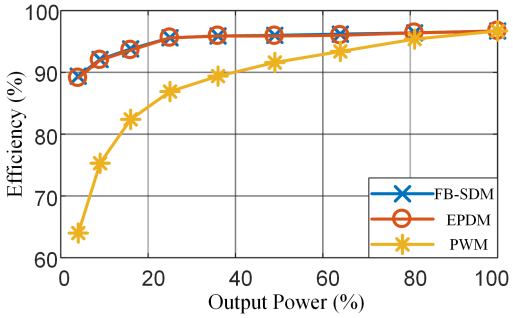

Fig. 14. Measured system efficiencies of FB-SDM, EPDM, and PWM.

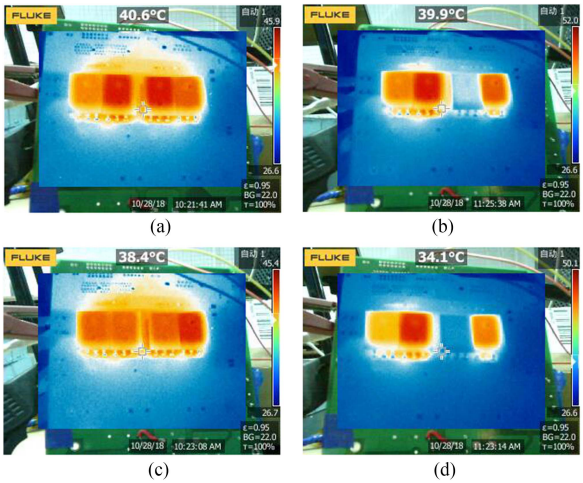

Fig. 15. Thermal performance between FB-SDM and EPDM. $\delta = 0.6$: (a) FB-SDM. (b) EPDM. $\delta = 0.4$: (c) FB-SDM. (d) EPDM.

Fig. 14. The efficiencies of FB-SDM and EPDM are almost equal because the ZVS condition is achieved in the full output range. The efficiency reaches above 90% over the power range from 10% to 100%. The efficiency of PWM is much lower than FB-SDM and EPDM because the inverter suffers from hard-switching.

The thermal performance between FB-SDM and EPWM is shown in Fig. 15. The results show that the losses of MOSFETs are more balanced in FB-SDM mode. The maximum temperature of MOSFETs in FB-SDM mode is 45.9 °C, and the maximum temperature of MOSFETs in EPDM mode is 52.0 °C.

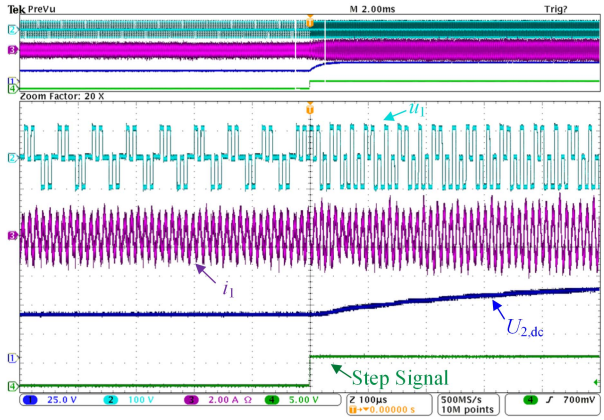

Fig. 16. Step response of FB-SDM from $\delta = 0.4$ to $\delta = 0.7$.

The EPDM inverter works on the half-bridge mode for $\delta = 0.4$, so the losses of a MOSFET is zero, which is shown in Fig. 15(d).

At last, the dynamic performance of FB-SDM is verified by experimental measurement. As shown in Fig. 16, it takes only several periods to increase the inverter output u_1 from 0.4 to 0.7. Thus, FB-SDM can regulate the inverter output voltage flexibly.

V. Conclusion

This letter proposes a new perspective of voltage step density on the power regulation for WPT systems, and an FB-SDM modulation scheme was proposed based on it. FB-SDM has the ability of balancing the power device losses and the minimum low frequency fluctuation. A modulator for generating drive signals of FB-SDM has been designed. The simulation and experimental results prove that FB-SDM performs better than other ZVS modulations and can replace them.

References

[1] R. Bosshard, U. Badstübner, J. W. Kolar, and I. Stevanović, "Comparative evaluation of control methods for inductive power transfer," in *Proc. IEEE Int. Conf. Renewable Energy Res. Appl.*, 2012, pp. 1–6.

[2] H. Fujita and H. Akagi, "Pulse-density-modulated power control of a 4 kW, 450 kHz voltage-source inverter for induction melting applications," *IEEE Trans. Ind. Appl.*, vol. 32, no. 2, pp. 279–286, Mar./Apr. 1996.

[3] W. Liu, K. T. Chau, C. H. T. Lee, X. Tian, and C. Jiang, "Hybrid frequency pacing for high-order transformed wireless power transfer," *IEEE Trans. Power Electron.*, vol. 36, no. 1, pp. 1157–1170, Jan. 2021.

[4] J. Tang, Q. Zhang, C. Cui, T. Na, and T. Hu, "An improved hybrid frequency pacing modulation for wireless power transfer systems," *IEEE Trans. Power Electron.*, vol. 36, no. 11, pp. 12365–12374, Nov. 2021.

[5] J. Tang, T. Na, T. Hu, and Q. Zhang, "Step density modulation for wireless power transfer systems," in *Proc. IEEE Int. Conf. Adv. Elect. Eng. Comput. Appl.*, 2021, pp. 110–114.

[6] H. Li, J. Fang, S. Chen, K. Wang, and Y. Tang, "Pulse density modulation for maximum efficiency point tracking of wireless power transfer systems," *IEEE Trans. Power Electron.*, vol. 33, no. 6, pp. 5492–5501, Jun. 2018.

[7] V. Esteve et al., "Enhanced pulse-density-modulated power control for high-frequency induction heating inverters," *IEEE Trans. Ind. Electron.*, vol. 62, no. 11, pp. 6905–6914, Nov. 2015.

[8] M. Fan, L. Shi, Z. Yin, L. Jiang, and F. Zhang, "Improved pulse density modulation for semi-bridgeless active rectifier in inductive power transfer system," *IEEE Trans. Power Electron.*, vol. 34, no. 6, pp. 5893–5902, Jun. 2019.

[9] V. Yenil and S. Cetin, "An improved pulse density modulation control for secondary side controlled wireless power transfer system using LCC-S compensation," *IEEE Trans. Ind. Electron.*, vol. 69, no. 12, pp. 12762–12772, Dec. 2022.